TITLE PAGE

Phenotypic appearances of Prostate utilizing PET-MR and PET-CT with ^{68}Ga PSMA, Radiolabelled Choline and ^{68}Ga DOTATATE

Athar Haroon[1,2], Asim Afaq [2], Soujanya Nuthakki[3], Alex Freeman [4], Lorenzo Biassoni[5], Stefano Fanti[6], Mohsen Beheshti[7], Hikmat Jan[1], Sobhan Vinjamuri[8], Mark Emberton[9], Jamshed Bomanji[10]

1-Barts Health NHS Trust, St Bartholomew's Hospital, Nuclear Medicine Department, London, UK
2-Institute of Nuclear Medicine, University College London Hospital NHS Trust
3-Aurora Health Care, Milwaukee WI, USA
4-Department of Pathology, University College London Hospital NHS Trust, UK
5-Great Ormond Street Hospital, London, UK
6-Department of Nuclear Medicine, University Hospital Sant'Orsola Malpighi, Bologna, Italy
7-St. Vincent's Hospital, Linz, Austria
8-Royal Liverpool and Broadgreen University Hospitals NHS Trust
9-Division of Surgery and Interventional Science, University College London, UK
10-Institute of Nuclear Medicine, University College London Hospitals NHS Trust, UK

Corresponding author:
Dr Athar Haroon MBBS, FRCR,

Consultant Radionuclide Radiologist
Nuclear Medicine Department
Barts Health NHS Trust
St Bartholomew's Hospital
London
UK
Email: **atharharoon@yahoo.com**

This work was undertaken at Barts Health NHS Trust, University College London Hospital, Great Ormond Street Hospital London and Aurora Health Care, Milwaukee WI, USA. The work carried out in UK was in collaboration with funding from UK Department of Health's NIHR Comprehensive Biomedical Research Centres and Cancer Research, United Kingdom. The authors have no financial disclosure of interest. An abstract of this work was presented at the Society of Nuclear Medicine and Molecular Imaging (SNMI) annual meeting in 2012 in Texas, USA.

ABSTRACT

OBJECTIVE:
To highlight the role of multimodality imaging and present differential diagnosis of abnormal tracer accumulation in the Prostate and periprostatic tissue.

METHOD:
Our departments have performed molecular imaging of the prostate utilising PET-CT and PET-MR with a range of biomarkers including ^{18}F FDG, radiolabelled Choline, ^{68}Ga DOTATATE PET-CT and ^{68}Ga PSMA images. We retrospectively reviewed the varying appearances of the prostate gland in different diseases and incidental findings in periprostatic region.

RESULTS:
The differential diagnosis of pathologies related to prostate and periprostatic tissue on multimodality imaging include

* Malakoplakia
* Rhabdomyosarcoma
* Lymphoma
* Prostate Cancer
* Neuroendocrine tumours
* Uchida changes
* Recto-prostatic fistula
* Synchronous malignancies
* Lymphocoele
* Schwanoma

CONCLUSION:
There exists a wide differential for abnormal tracer accumulation in the prostate gland. As a radiologist and nuclear medicine physician it is important to be aware of range of prostatic and periprostatic pathologies.

Phenotypic appearances of Prostate utilizing PET-MR and PET-CT with ^{68}Ga PSMA, Radiolabelled Choline and ^{68}Ga DOTATATE

INTRODUCTION

Prostate cancer has a diverse range of findings and it can present as small indolent intra-prostatic lesion to highly aggressive disseminated disease. Biological heterogeneity presents a diagnostic challenge and it is important to understand the underlying mechanism of spread of prostate cancer. A reporting radiologist or nuclear medicine physician should be aware of varying appearances of prostate at different stages and spectrum of findings with different biomarkers utilizing PET-CT or PET-MRI. We validated our findings on the PET-CT appearances of prostate cancer presenting as focal or diffuse uptake (1) (2) (3). This article relates to the phenotypic appearances of the prostate with a range of biomarkers which facilitate diagnosis of prostate cancer and these can be categorized into different groups:

1-Increased choline kinase activity (^{18}F Methyl Choline, ^{18}F Ethyl Choline and ^{11}C Choline)

2-Prostate specific membrane proteins (^{68}Ga PSMA)

3-Receptor imaging (^{68}Ga DOTATATE)

4-Glucose imaging (^{18}F FDG)

BIOMARKERS

1-Radiolabelled Choline

There is increased proliferation of cells in cancer with increased Choline Kinase activity. This enzyme is important for phosphorylation and choline uptake is increased as a result of this. There are three radiolabelled sub-types of Choline (^{18}F Methyl Choline, ^{18}F Ethyl Choline and ^{11}C Choline). Normal biodistribution of these three subtypes of radiolabelled Choline has been described by Athar Haroon et al (4). Visceral localization of radiolabelled Choline is the same for all subtypes. There are only minor differences which fall in the category of statistically significant or non significant differences. Range of SUVs for various organs for the three tracers was also evaluated in this study. The main utility of radiolabelled Choline PET is in detection of biochemical relapse of prostate cancer (2).

2-^{68}Ga Prostate Specific Membrane Antigen (PSMA)

PSMA is present in prostate epithelial cells, salivary glands, renal tubular cells, small intestine and coeliac ganglia. Three properties of PSMA makes it a highly attractive target for imaging (a) Increased expression in Prostate cancer cells (b) Cell membrane anchorage (c) Internalization. ^{68}Ga PSMA is more sensitive and specific than radiolabelled Choline in patients with recurrent prostate cancer (5).

3- 2-[^{18}F]-fluoro-2-deoxy-D-glucose (^{18}F-FDG)

^{18}F FDG is a radiolabelled analog of glucose and it also uses transmembrane glucose transporters to enter a cell which is phosphorylated by hexokinase. As ^{18}F FDG demonstrates low uptake in newly diagnosed prostate cancer, it is of only limited value for local staging of prostate cancer.

4- ^{68}Ga-DOTATATE

Somatostatin is a cyclic neuropeptide and it is found in neurons and endocrine cells. There are five subtypes of somatostatin receptors which may frequently co-exist in same cell. There is overexpression of sstr in prostate cancer and 30% of prostate cancer cells (6) express sstr. ^{68}Gallium (^{68}Ga) 1,4,7,10-tetraazacyclododecane-1,4,7,10-tetraaceticacid(DOTA)-octreotate (DOTATATE,GaTate) PET-CT allows cell surface expression of somatostatin receptors (SSRRs).

DIFFERENTIAL DIAGNOSIS

1-MALAKOPLAKIA:

Malacoplakia is derived from Greek words “malakos” meaning “soft” and “plakos” meaning “plaque” and the first person to coin this term was Von Hansemann. Malacoplakia is a chronic inflammatory condition with different etiologies including tuberculosis, tumours, fungal infections, parasitic infestations, sarcoidosis, ectopic rests of adrenal cortical cells and coliform infections. Histological hallmark are Von Hansemann cells and Michaelis-Gutamann bodies. Clinically, genitourinary tract is the most common site with 80-90% of patients having coliform infection.

CASE STUDY:

A 71 years old man of Caribbean origin presented with proximal muscle weakness and sensory loss in all four limbs. His ESR was 100. His treponemal antibody enzyme-linked immunosorbent assay (*ELISA*) was positive (syphilis), rapid plasma reagin (RPR) was positive at a titre of 4 and t*reponema pallidum particle agglutination* assay (*TPPA)* was also positive. Sural nerve biopsy was in keeping with segmental demyelination with axonal degeneration. A diagnosis of chronic inflammatory demyelinating neuropathy

was made. ^{18}F FDG PET-CT (FIG 1) showed a non-avid lung lesion. There was a single focus of FDG uptake at the right lateral aspect of the prostate and on biopsy malakoplakia was confirmed.

2-RHABDOMYOSARCOMA

Prostatic sarcomas are rare and arise from mesoderm and constitute 0.7% of the primary tumours of the prostate (7). There is increased risk of local recurrence in patients with genitourinary sarcomas when compared with sarcomas of the soft tissues (8) (9). In paediatric population RMS with localised and metastatic disease have better prognosis (10). AJCC has re-categorized nodal involvement from stage IV to stage III due to better prognosis (10). MRI with superior anatomical resolution and PET providing additional information about the nodal and distant status of disease can help triaging patients for surgery.

CASE STUDY:

An 18 months old boy presented with urinary outflow obstruction and bilateral hydronephrosis. MRI and ^{18}F FDG PET-CT scan (FIG 2) demonstrated soft tissue mass bulging into the bladder displacing it anteriorly and was adherent to the rectum. Histology demonstrated embryonic rhabdomyosarcoma with anaplasia localised to the bladder neck and prostate. He was treated with chemotherapy and follow-up PET-CT scan short residual low-grade uptake in the primary mass lesion with no evidence of metabolically active metastatic disease.

3- LYMPHOMA

These are low-grade malignancies and the incidence is highest in the seventh decade (11) (12) (3) (4). Following features raise the possibility of primary lymphoma of the prostate (11)

(a) Symptoms related to prostatic enlargement.

(b) Predominant site of involvement is prostate.

(c) Absence of involvement of liver, spleen and lymph nodes (1 month of diagnosis)

^{18}F FDG PET-CT provide additional information as it is possible to differentiate these from Diffuse large B cell lymphoma (13) on histology.

a) High grade adenocarcinoma shows nuclear pleomorphism, cellular cohesion with large sheets of tumor cells. On the other hand infiltrative adenocarcinoma are more difficult to distinguish. Most of the adenocarcinomas are negative for CD45, CD20 while diffuse large B cell lymphoma demonstrates positivity with such immunoprofile (12).

b) Urothelial carcinomas show cellular cohesion including solid tumor nests and non invasive carcinoma on the surface urothelium. There exists an overlap with diffuse large B cell lymphoma with extreme morphological diversity, invasive, discohesive tumor cells. Urothelial carcinomas are positive for pancytokeratin, CK903/34BE12, p63 and GATA3 5-7. These are negative for CD45 and CD20.

c) Small cell carcinoma show sheet like growth, small blue cells with scant cytoplasm, high nuclear to cytoplasmic ratio, salt and pepper chromatin, nuclear molding, single cell or geographic necrosis. Small cell carcinomas express pancytokeratin, chromogranin and

synaptophysin. These lack CD45 and CD20.

4-PROSTATE CANCER

Acinar adenocarcinoma

Adenocarcinomas (FIG 3, FIG 4) are the most common type of prostate cancer. It develops in the gland cells that line the prostate (14). Ductal adenocarcinoma starts in the cells that line the ducts (tubes) of the prostate gland. It tends to grow and spread more quickly than acinar adenocarcinoma. When uptake pattern of ^{18}F Ethyl Choline PET-CT was correlated with MR Template guided mapping biopsies it was found that 60 minutes imaging was more sensitive than 90 minutes imaging for detection of clinically significant prostate cancer (2).

Transitional cell (or urothelial) cancer

Transitional cell cancer of the prostate starts in the cells that line the tube carrying urine to the outside of the body (the urethra). There is more than 50%, 5 year disease specific survival rate for patients with transitional cell carcinoma of the prostate (15) and it was found that the extent of loco-regional spread was the strongest rate predictor of patient survival outcome.

Squamous cell cancer

These cancers develop from flat cells that cover the prostate. They tend to grow and spread more quickly than adenocarcinoma of the prostate. These are extremely rare comprising only 0.5-1% of all prostatic carcinomas (16).

Small cell prostate cancer

Small cell prostate cancer is made up of small round cells. It's a type of neuroendocrine

cancer (14). These are rare and can be mistaken for high-grade conventional prostate carcinoma. It has poor prognosis.

5- NEUROENDOCRINE TUMORS OF THE PROSTATE

Primary neuroendocrine carcinomas are divided into two main types

(a) High grade histological type (small cell carcinoma)

(b) Low grade histological type (carcinoid tumors) (17).

Prostate carcinoid are associated with adenocarcinomas(18), trans-differentiation from adenocarcinomas (19) and multiple endocrine neoplasia (20). These lesions pose diagnostic challenge due to several overlapping features such as adenocarcinomas may demonstrate neuroendocrine features (carcinoid like growth pattern) and may show positive immunostaining for neuroendocrine markers (21). It is of crucial importance to know whether the cancer is conventional adenocarcinoma with neuroendocrine differentiation or a true neuroendocrine carcinoma.

In a study by Shastry et al (22) distribution pattern of ^{68}Ga DOTATATE in disease free patients was evaluated and the uptake was found to be low grade and diffuse in the prostate. There is low density of sst2 receptors in normal prostate gland in the smooth muscles.

CASE STUDY

A male patient with calcified mass in the tail of the pancreas with intense somatostatin receptor expression was diagnosed as pancreatic neuroendocrine tumour on histology. There were multiple tracer avid metastatic deposits in the liver (FIG 5) and also periportal lymph nodes. The images of the pelvis showed heterogeneous tracer uptake in

in the central gland of prostate.

6- UCHIDA CHANGES

High frequency focused ultrasound (HIFU) utilizes the physical properties of ultrasound. When it is used for therapy it can be focused by an acoustic lens, a transducer or electronic phased array. This creates zones of high and low pressure through the tissues and this causes thermal coagulation and/or acoustic cavitation (23). On PET-CT scan it is difficult to identify changes on the low dose CT as the focal point is small (10mm x 1-2mm) and is situated along the long axis of the beam. These changes are called "Uchida changes" (24) and were described by Professor Toyoaki Uchida in Japan. There are three grades I- changes identified within the treatment zones. II-confluent between the adjacent treatment zones and III-migration outside the treatment zone. The changes are further sub-classified into three types based on the involvement of the focal regions. (a) <10% (b) 10-50% (c) >50%. The overall impact of treatment results in altered morphology of the gland, which are very difficult to recognise on the low dose PET-CT with formation of subsequent scar tissue. If MRI is available then anatomical alteration particularly "Uchida changes" should be evaluated. Cavitation, fistulation (FIG 6) and asymmetrical atrophic changes should be considered before labelling tracer avid disease site as tumor. Excreted activity due to focal small cavitation adjacent to the urethra may accumulate urinary activity and can be misdiagnosed as a metabolically active pathological lesion.

7- POST RADIOTHERAPY

The main utility of PET is detection of early biochemical relapse. Novel biomarkers have the potential to discriminate viable disease versus post surgical and post radiotherapy changes (25). In post radiotherapy scenario there is relatively poor yield of FDG and

Choline with PSA less than 4 ng/ml (26). The most common reason for false positive result is post radiotherapy-related inflammatory change.

CASE STUDY:

A 72 years old man with history of prostate cancer presented with biochemical relapse (PSA 12.67). The patient underwent ^{18}F Choline PET-CT which showed a moderate intensity focal uptake in the right lobe of the prostate gland and no evidence of tracer avid disease in the contralateral lobe. The patient underwent MR-Template guided biopsy of the prostate which showed only fibrosis on the right side and Gleason 3+4 adenocarcinoma of the prostate on the left side. The scan was false positive in the right lobe and false negative in the left lobe.

8-POST HORMONES

Hormones suppress the choline uptake of prostate cancer. There are limited studies which have evaluated this effect. It is recommended that androgen deprivation therapy should be put on hold prior to choline PET-CT to avoid false negative outcome (27). This is of utmost importance in clinical scenario of biochemical relapse of prostate cancer in hormone naïve patients.

9-POST TRANSURETHRAL RESECTION OF THE PROSTATE (TURP)

Trans-urethral resection of the prostate causes increase in the diameter of the prostatic urethra. The prostatic urethra appears capacious with focal intense uptake when delayed imaging with ^{18}F FDG or when radiolabelled Choline is used. The intensity of uptake matches that of the excreted activity in the urinary bladder.

10- POST PROSTATECTOMY

Radical prostatectomy is the removal of entire prostate gland. The modern methods encourage the use of nerve sparing surgery to preserve the erectile function. Prostatectomy involves partial or complete removal of the prostate. PET-CT readers should be aware of two surgical approaches, as postoperative scarring will alter the morphology of the prostate bed and perineum. Functional imaging helps to distinguish scar tissue from tumour recurrence or metastases (Fig 7).

11-RECTO-PROSTATIC FISTULA:

Recto-prostatic fistula are either due to inflammatory etiologies (abscess formation, xanthogranulomatous prostatitis), iatrogenic (post surgical, brachytherapy, high frequency focused ultrasound) or related to primary prostate cancer (28).

CASE STUDY:

A patient presented with left sided hydronephrosis and hydroureter. Investigations revealed left VUJ obstruction. MRI demonstrated a large prostate cancer with infiltration of the left lateral aspect of the pelvis and fistula formation with rectum. ^{18}F Choline PET-CT showed a heterogenous appearing mass with photopenic areas (FIG 8). A right lower lobe lung nodule was demonstrated and it was intensely avid on ^{18}F FDG PET-CT. On original histology it was thought to be due to small cell carcinoma of the lung. On PSMA staining diagnosis of metastases from prostate cancer was confirmed. This patient demonstrated significant progression on bone scan with development of osteoblastic bone metastases within an interval of 6 months.

12-SYNCHRONOUS MALIGNANCIES

(a) PROSTATE AND SKIN CANCER

There is 1% incidence of skin metastases in patients with prostate cancer (29) and of note there is increased risk of melanoma after prostate cancer treatment (29). At our institute, a patient who was being investigated for suspected relapse of the prostate cancer had ^{18}F Choline PET-CT which demonstrated relapse at the mid gland and left lobe. An intensely avid nodule was noted at the left shoulder, which was clinically thought to be skin metastases from prostate cancer. The biopsy was confirmed to be squamous cell carcinoma of the skin.

(b) PROSTATE AND RECTAL CARCINOMA

We came across a patient who had ^{18}F Choline PET-CT as part of work up for prostate cancer relapse. There was focal area of intense uptake in the rectum at the left lateral wall. On retrospective review of the MRI, it was found to be a nodular lesion situated at the lateral wall of the rectum. It was difficult to detect it initially on zoomed narrow field of view images but on direct inspection it was found to be a rectal carcinoma incidentally detected on MRI and Choline PET-CT.

13-SCHWANOMA

Benign tumours originating from the neuronal sheath are known as neurilemmomas or schwanomas. These occur along the distribution of the cranial nerves and in the flexor surfaces of the upper and lower extremeties. Most of these are incidently detected as part of staging.

14- LYMPHOCOELE

These are collections of fluid secondary to disruption and surgical dissection of the lymphatics and lymph nodes. These are not metabolically active unless there is an inflammatory reaction. Low dose CT detects these as hypodense area with well defined margins.

CONCLUSION

It is concluded that there exists a wide differential for prostatic and periprostatic pathologies. As a nuclear medicine physician it is important to be aware of the range of prostatic and periprostatic pathologies. Biological heterogeneity presents a diagnostic challenge in detection of Prostate Cancer. Choline uptake in the cells can be due to inflammation, prostatic hyperplasia and malignancy. PSMA is present in prostate epithelial cells, renal tubular cells and coeliac ganglia. 30% of Prostate cancer show over-expression of Somatostatin receptors. Malacoplakia can be due to tuberculosis, sarcoidosis, tumours and fungal infections. When reporting PET for evaluation of prostate cancer, reporting nuclear medicine physician should evaluate morphology of the prostate gland particularly in cases where previous treatment has been given, check pelvis and other nodal stations for involvement and assess for the presence of incidental findings.

REFERENCES:

1. Haroon A, Almuhaideb A, Dickson J, Ahmed H, Syed R, Kirkham A, et al. Dual phase 18F-FDG PET-CT imaging in evaluation of "radio-recurrent" prostate cancer. J Nucl Med. 2011 May 1;52(supplement 1):1901–1901.

2. Haroon A, Ahmed HU, Cathcart P, Almuhaideb A, Kayani I, Dickson J, et al. (18)F-FECH PET-CT to Assess Clinically Significant Disease in Prostate Cancer: Correlation With Maximum and Total Cancer Core Length Obtained via MRI-Guided Template Mapping Biopsies. AJR Am J Roentgenol. 2016 Dec;207(6):1297–306.

3. Haroon A, Almuhaideb A, Dickson J, Emberton M, Kayani I, Ahmed H, et al. 18F Choline PET-CT for assessing disease recurrence: Correlation with TRUS, MR template-guided prostate mapping biopsies. J Nucl Med. 2012 May 1;53(supplement 1):1415–1415.

4. Haroon A, Zanoni L, Celli M, Zakavi R, Beheshti M, Langsteger W, et al. Multicenter study evaluating extraprostatic uptake of 11C-choline, 18F-methylcholine, and 18F-ethylcholine in male patients: physiological distribution, statistical differences, imaging pearls, and normal variants. Nucl Med Commun. 2015 Nov;36(11):1065–75.

5. Afshar-Oromieh A, Haberkorn U, Schlemmer HP, Fenchel M, Eder M, Eisenhut M, et al. Comparison of PET-CT and PET/MRI hybrid systems using a 68Ga-labelled PSMA ligand for the diagnosis of recurrent prostate cancer: initial experience. European journal of nuclear medicine and molecular imaging. 2014;41(5):887–97.

6. Luboldt W, Zöphel K, Wunderlich G, Abramyuk A, Luboldt H-J, Kotzerke J. Visualization of somatostatin receptors in prostate cancer and its bone metastases with Ga-68-DOTATOC PET-CT. Mol Imaging Biol. 2010 Feb;12(1):78–84.

7. Wang X, Liu L, Tang H, Rao Z, Zhan W, Li X, et al. Twenty-five cases of adult prostate sarcoma treated at a high-volume institution from 1989 to 2009. Urology. 2013 Jul;82(1):160–5.

8. Dotan ZA, Tal R, Golijanin D, Snyder ME, Antonescu C, Brennan MF, et al. Adult genitourinary sarcoma: the 25-year Memorial Sloan-Kettering experience. J Urol. 2006 Nov;176(5):2033–8; discussion 2038–9.

9. Sexton WJ, Lance RE, Reyes AO, Pisters PW, Tu SM, Pisters LL. Adult prostate sarcoma: the M. D. Anderson Cancer Center Experience. J Urol. 2001 Aug;166(2):521–5.

10. Edge SB, Compton CC. The American Joint Committee on Cancer: the 7th edition of the AJCC cancer staging manual and the future of TNM. Ann Surg Oncol. 2010 Jun;17(6):1471–4.

11. Bostwick DG, Mann RB. Malignant lymphomas involving the prostate. A study of 13 cases. Cancer. 1985 Dec 15;56(12):2932–8.

12. Chuang A-Y, DeMarzo AM, Veltri RW, Sharma RB, Bieberich CJ, Epstein JI. Immunohistochemical differentiation of high-grade prostate carcinoma from urothelial carcinoma. Am J Surg Pathol. 2007 Aug;31(8):1246–55.

13. Warrick JI, Owens SR, Tomlins SA. Diffuse large B-cell lymphoma of the prostate. Arch Pathol Lab Med. 2014 Oct;138(10):1286–9.

14. Types and grades | Cancer Research UK [Internet]. [cited 2016 Dec 26]. Available from: http://www.cancerresearchuk.org/about-cancer/prostate-cancer/types-grades

15. Cheville JC, Dundore PA, Bostwick DG, Lieber MM, Batts KP, Sebo TJ, et al. Transitional cell carcinoma of the prostate. Cancer. 1998 Feb 15;82(4):703–7.

16. Mohan H, Bal A, Punia RPS, Bawa AS. Squamous cell carcinoma of the prostate. International Journal of Urology. 2003 Feb 1;10(2):114–6.

17. Nelson EC, Cambio AJ, Yang JC, Ok J-H, Lara PN, Evans CP. Clinical implications of neuroendocrine differentiation in prostate cancer. Prostate Cancer Prostatic Dis. 2006 Oct 31;10(1):6–14.

18. Montasser AY, Ong MG, Mehta VT. Carcinoid tumor of the prostate associated with adenocarcinoma. Cancer. 1979;44(1):307–10.

19. Stratton M, Evans DJ, Lampert IA. Prostatic adenocarcinoma evolving into carcinoid: selective effect of hormonal treatment? Journal of clinical pathology. 1986;39(7):750–6.

20. Whelan T, Gatfield CT, Robertson S, Carpenter B, Schillinger JF. Pediatric Articles: Primary Carcinoid of the Prostate in Conjunction With Multiple Endocrine Neoplasia IIb in a Child. The Journal of urology. 1995;153(3):1080–2.

21. Almagro UA, Tieu TM, Remeniuk E, Kueck B, Strumpf K. Argyrophilic,'carcinoid-like'prostatic carcinoma. An immunocytochemical study. Archives of pathology & laboratory medicine. 1986;110(10):916–9.

22. Shastry M, Kayani I, Wild D, Caplin M, Visvikis D, Gacinovic S, et al. Distribution pattern of 68Ga-DOTATATE in disease-free patients: Nuclear Medicine Communications. 2010 Oct;1.

23. Illing RO, Leslie TA, Kennedy JE, Calleary JG, Ogden CW, Emberton M. Visually directed high-intensity focused ultrasound for organ-confined prostate cancer: a proposed standard for the conduct of therapy. BJU International. 2006 Dec 1;98(6):1187–92.

24. Uchida T, Ohkusa H, Nagata Y, Hyodo T, Satoh T, Irie A. Treatment of localized prostate cancer using high-intensity focused ultrasound. BJU Int. 2006 Jan;97(1):56–61.

25. Boukaram C, Hannoun-Levi J-M. Management of prostate cancer recurrence after definitive radiation therapy. Cancer Treatment Reviews. 2010 Apr;36(2):91–100.

26. Greco C, Cascini GL, Tamburrini O. Is there a role for positron emission tomography imaging in the early evaluation of prostate cancer relapse? Prostate Cancer Prostatic Dis. 2008 Jan 8;11(2):121–8.

27. Dost RJ, Glaudemans AWJM, Breeuwsma AJ, Jong IJ de. Influence of androgen deprivation therapy on choline PET-CT in recurrent prostate cancer. Eur J Nucl Med Mol Imaging. 2013 Jul 1;40(1):41–7.

28. Xing L, Liu Z, Deng G, Wang H, Zhu Y, Shi P, et al. Xanthogranulomatous prostatitis with prostato-rectal fistula: a case report and review of the literature. Res Rep Urol. 2016 Sep 16;8:165–8.

29. Brownstein MH, Helwig EB. Metastatic tumors of the skin. Cancer. 1972 May;29(5):1298–307.

Figures

Malakoplakia:

(a) (b)

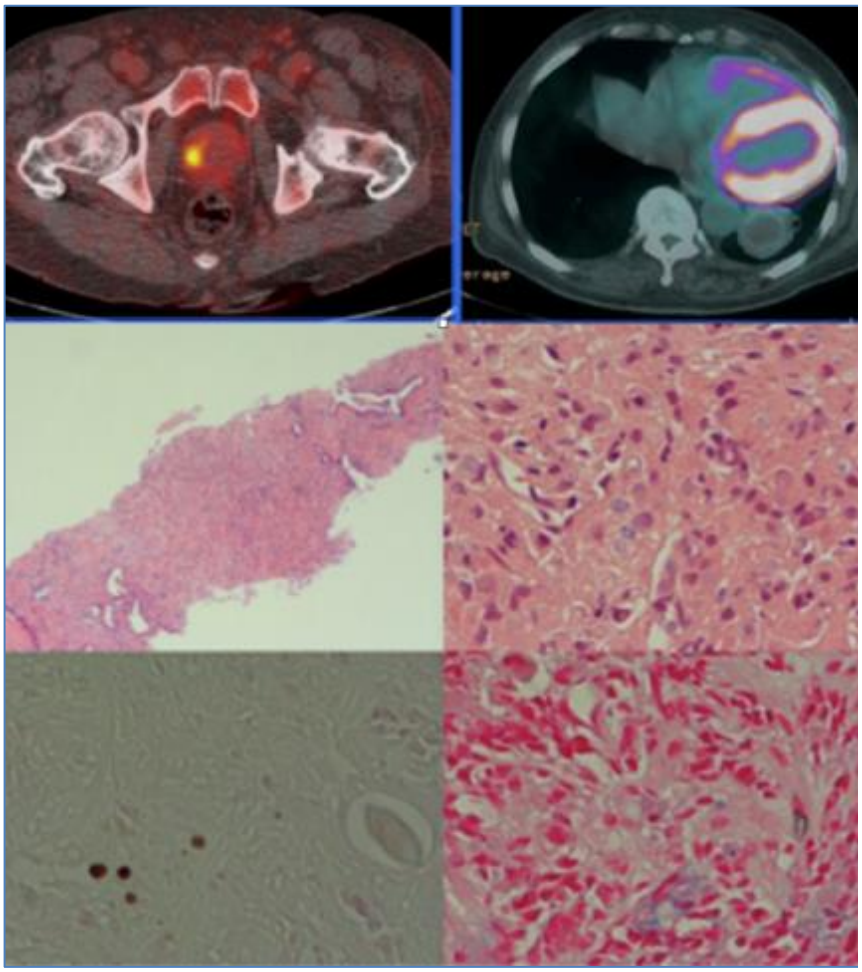

(c) (d)

(e) (f)

Fig: 1 **(a)** ^{18}F FDG Axial fused PET/CT showing a focal area of increased uptake involving the right lobe of the prostate gland. **(b)** A well-circumscribed area of peripheral increased soft tissue density and only faint uptake at the left lung base. **(c)** H&E stain x 40 magnification **(d)** H&E stain with Michaelis-Guttman body x 400 magnification **(e)** von Kossa stain for calcium x 400 magnification **(f)** Perls stain for iron x400 magnification

Rhabdomyosarcoma:

CASE STUDY:

(a) **(b)** **(c)**

Fig 2: (a) Sagittal fused PET CT and low dose CT image showing a heterogenous mass infiltrating the superior aspect of the prostate gland and extending to the presacral region. The urinary bladder is compressed (catheter balloon insitu). The mass demonstrates low-grade metabolic activity and compresses the urinary bladder anteriorly. Sagittal T2 weighted image show heterogenous signal intensity. Histology confirmed this to be rhabdomyosarcoma.

Primary Prostate Cancer

Acinar adenocarcinoma

(a)

(b)

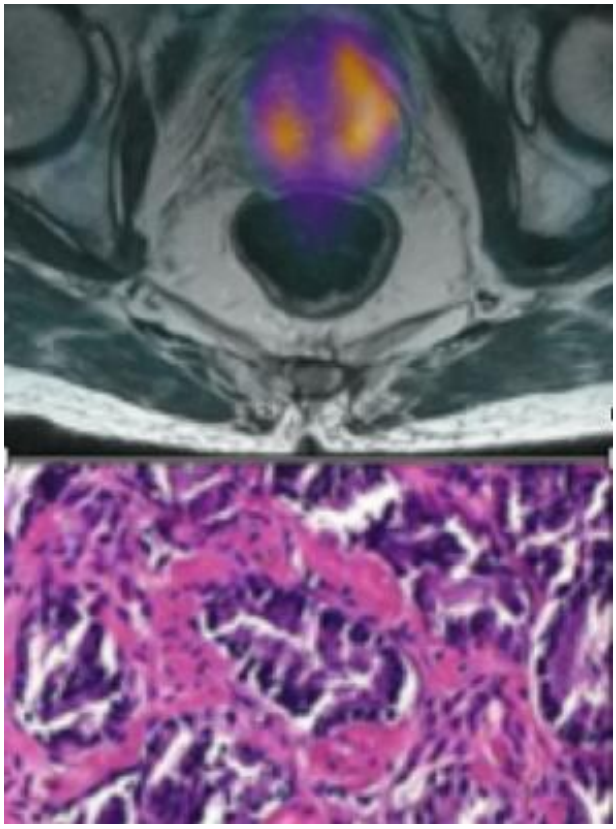

Fig 3: (a) ^{18}F Choline PET/MRI showing focal uptake in the right lobe and diffuse pattern is seen in the left lobe. Histology confirming poorly differentiated adenocarcinoma in abnormal areas of PET CT (Gleason 4+4)

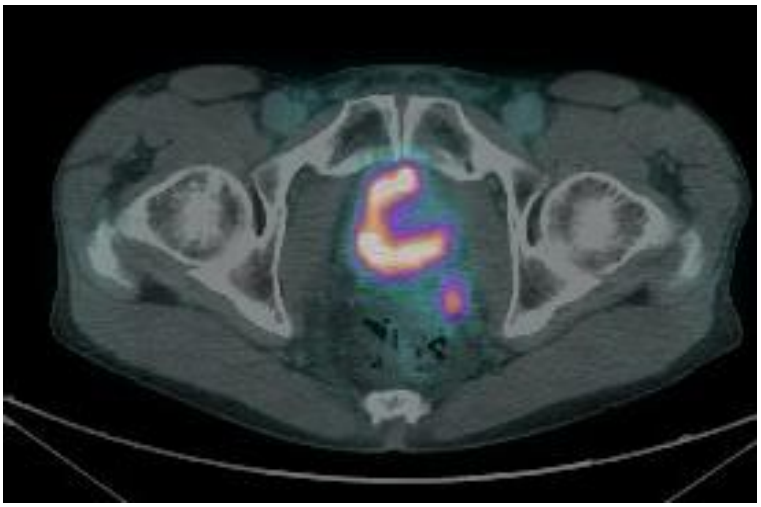

Fig 4: Rising PSA was noted in a patient with previous history of prostate cancer, left seminal vesicle involvement, which was removed at surgery and then treated with radiotherapy. ^{68}Gallium PSMA PET/CT showed focal area of uptake at the poster aspect of the bladder on the left side with soft tissue abnormality on the low dose CT. This is in keeping with disease relapse.

NEUROENDOCRINE TUMORS OF THE PROSTATE

CASE STUDY:

(a) (b)

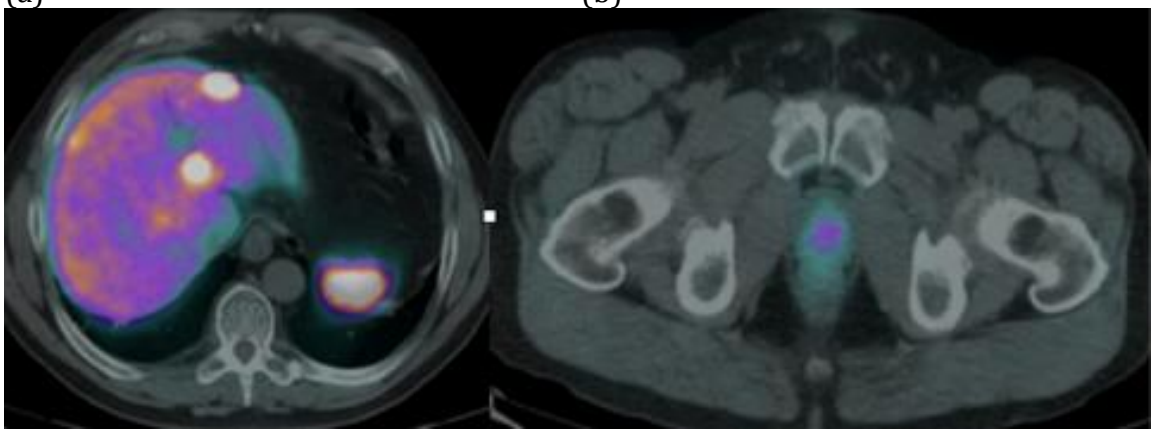

Fig 5: (a) ^{68}Gallium Octreotate axial fused PET/CT (upper abdomen and pelvis) image in a patient with metastatic pancreatic neuroendocrine tumor. There are multiple tracer avid liver metastastases. (b)In addition there is focal intense Somatostatin receptor expression in the prostate gland.

UCHIDA CHANGES

(a)

(b)

(c)

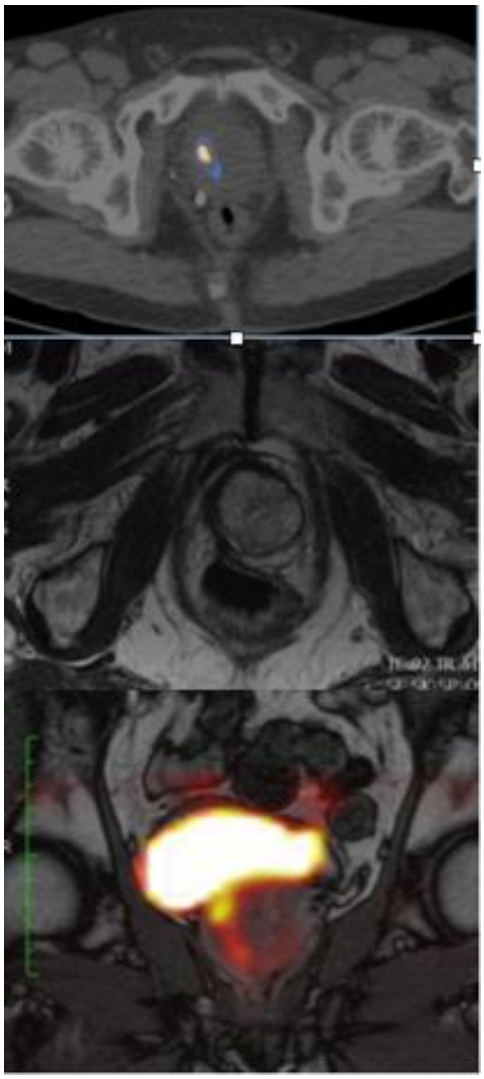

Fig 6: (a) Axial ^{18}F Choline PET/CT demonstrating focal area of apparent increased uptake in the right lobe of the prostate gland. Axial MRI showed post HIFU changes with marked atrophy of right lobe, hypertrophy of the left lobe. Coronal fused PET/MRI showed urethral tract with excreted activity and no evidence of tumour.

PERINEAL METASTASES

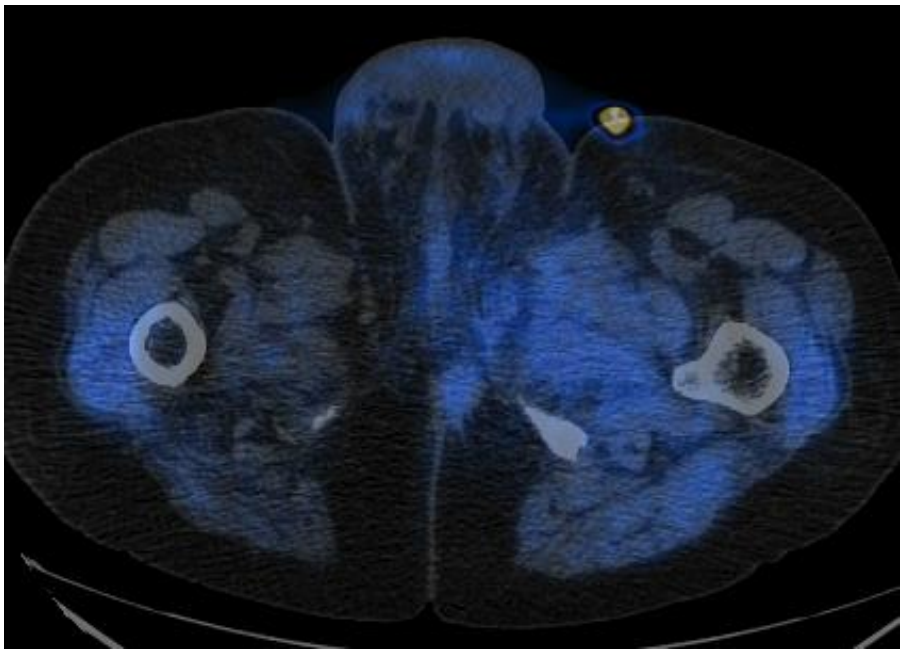

Fig 7: ^{18}F Choline axial fused PET/CT images in a patient post radical prostatectomy . There is a speculated mildly avid soft tissue abnormality in the left ischio-rectal fossa, which was a metastatic deposit from prostate cancer. Focal intense uptake at the left inguinal region is excreted activity in the drainage tube of urinary catheter.

RECTO-PROSTATIC FISTULA:

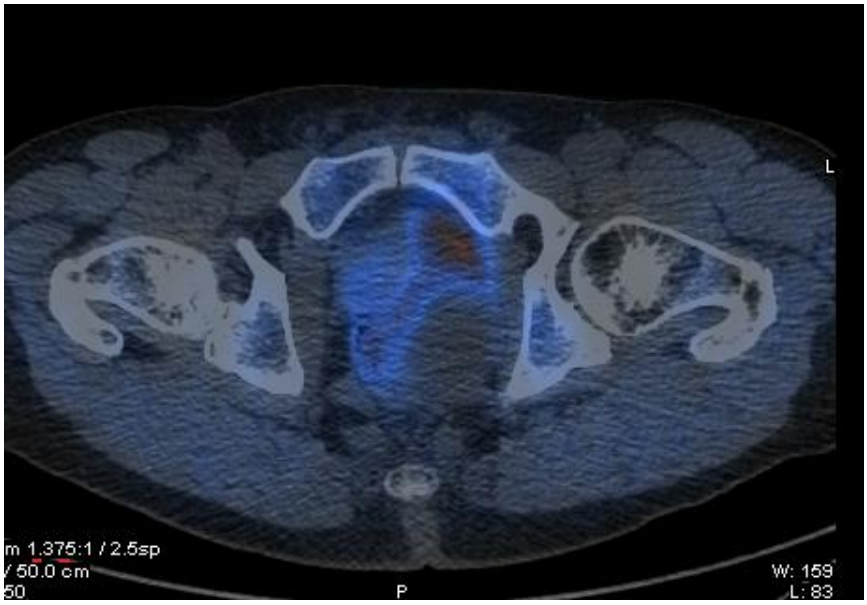

Fig 8: Axial fused ^{18}F Choline PET/CT showing heterogeneously avid soft tissue involving the prostate with multiple photopenic areas and soft tissue mass extending into the lateral aspect of the prostate gland.

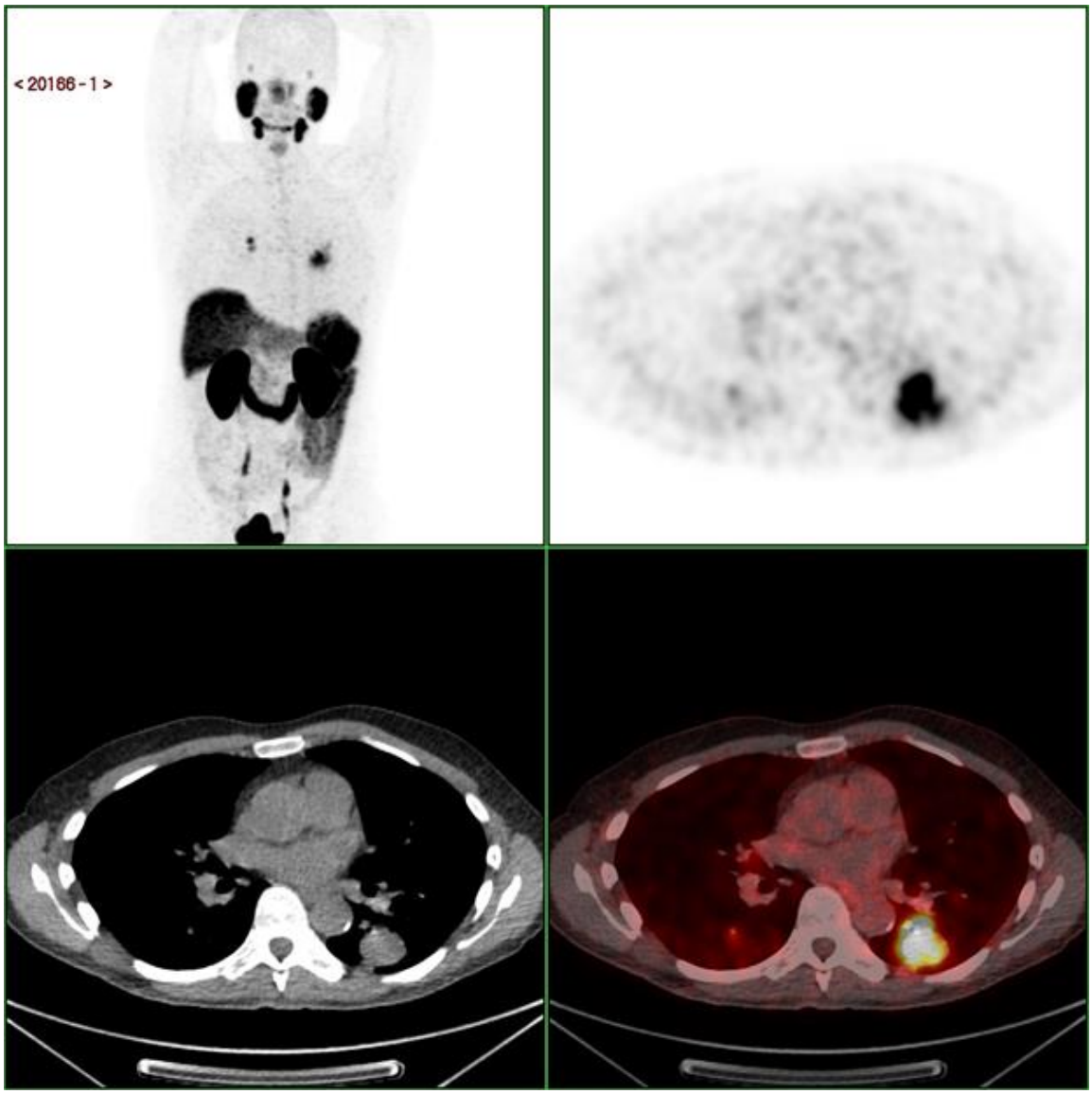

Fig 9: ^{68}Ga PSMA PET/CT MIP, axial PET, low dose CT and PET/CT in a 75 years old patient with biochemical relapse following radiotherapy (PSA 9.2). There are bilateral lung nodules, largest in the apical segment of the left lower lobe with intense tracer uptake. These findings are in keeping with metastatic disease.